Eur. Phys. J. B **19**, 49–63 (2001)

THE EUROPEAN PHYSICAL JOURNAL B

EDP Sciences
© Società Italiana di Fisica
Springer-Verlag 2001

Geometrical approach for the mean-field dynamics of a particle in a short range correlated random potential

F. Thalmann[a]

LEPES-CNRS, Laboratoire associé à l'UJF-Grenoble, BP166X, 25 avenue des Martyrs, 38042 Grenoble Cedex, France
and
Department of Physics and Astronomy, University of Manchester, Oxford Road, Manchester M13 9PL, UK

Received 7 May 2000 and Received in final form 22 August 2000

Abstract. We consider the zero temperature relaxational dynamics of a particle in a random potential with short range correlations. We first obtain a set of "two-times" mean-field equations (including the case of a finite, constant, driving force), and we present detailed results coming from a numerical integration of these equations. We restrict ourselves to the situation where the spatial correlations of the random potential decrease exponentially (otherwise our geometrical analysis fails). It is possible, in this case, to compute the spectrum of the Hessian of the energy landscape, and we subsequently propose a geometrical description of the "mean field aging" behavior. Our numerical results combined with further analytical arguments finally lead to the waiting-time dependence of the main characteristic time scales.

PACS. 05.70.Ln Nonequilibrium and irreversible thermodynamics – 64.70.Pf Glass transitions – 75.10.Nr Spin-glass and other random models

1 Introduction

The understanding of the out-of-equilibrium dynamics of glassy systems, including spin glasses, structural glasses, superconductor vortex glasses... , is a challenging problem.

Much of the current knowledge in this field originates from the study of mean field models like, for instance, the Sherrington-Kirkpatrick spin glass [1]. The spherical p-spin model is such a model, with a closed set of equations for the correlation functions of the dynamical variables, or "soft spins" [2,3]. In the thermodynamical limit, each spin is coupled to an infinity of other spins, and each spin fluctuates independently in the effective environment created by all the other spins. As a consequence, the dynamics simplifies drastically, and reduces to a few correlation functions, to be determined self-consistently, which completely characterize the Gaussian fluctuations of all dynamical variables. This is the "dynamical mean-field solution" of the model.

The mean-field dynamics of this model has proved extremely rich, its most striking feature being the existence of a non-trivial aging relaxation regime at low temperatures [3]. For instance, the solution of the mean field equations in this out-of-equilibrium regime establishes the existence of a generalised fluctuation-dissipation theorem (*i.e.* connecting correlation and response functions) which has since been observed in the simulations of more realistic, finite dimensional systems [4]. Then, the mean field approach gives a valuable insight on the experimentally observed aging behavior of disordered magnetic systems [5]. Finally, the dynamics of the p-spin glass model is of prime importance because of its close connection with the "mode coupling" description of structural glasses [6].

However, a crucial shortcoming of this mean-field description, is its inability to properly take into account the thermally activated motion over the potential energy barriers at low temperatures, leading to a sharp dynamical transition – divergence of a relaxation time – whereas the corresponding "finite dimensional" behaviour is just a progressive slowing down of the dynamics.

Despite this, the mean field dynamics remains a major issue in the study of the out-of-equilibrium statistical physics of disordered systems, and any physical insight on its aging mechanism is of interest. A major step in that direction was made by Kurchan and Laloux [7] who investigated the zero temperature relaxation of various systems, including ferromagnets and spin glasses. The zero temperature limit makes it possible to consider the energy landscape, rather than an ill defined "free-energy" landscape, without reducing the dynamics to something trivial.

In this work, we further extend their approach, and apply it to another interesting system: the mean-field dynamics of a particle in a short-range correlated random potential. The out-of-equilibrium, aging dynamics of this model was studied first in [8], and thoroughly investigated in [9], showing that this model belongs to the same universality class as the spherical p-spin model.

[a] e-mail: fabrice@theory.ph.man.ac.uk

What makes this model very interesting is its natural extension, when a finite and constant external force is applied to the particle. Then, it becomes a paradigm of the "driven glassy system", situation where a non-linear response to the force as well as a significant violation of the fluctuation-dissipation theorem are expected, as shown by Horner [10].

In this paper, we derive the dynamical mean field equations in the presence of a constant force. These equations are then numerically solved, both in the absence and in the presence of a weak external force, restricting ourselves to the linear response regime. Then, we start our geometrical analysis of the zero temperature relaxation by a simple random matrix calculation that we believe to describe satisfactorily the Hessian of an exponentially correlated Gaussian potential (while it fails for other kinds of correlations). Next, we perform an "instantaneous normal mode" analysis of the relaxational motion. The key observable turns out to be the (intensive) energy difference between the energy $\mathcal{E}(t)$ at a given time t, and its asymptotic value $\mathcal{E}(t=\infty)$. We subsequently analyse the waiting time dependence of two characteristic time scales t_f, t_b, that we relate to $\mathcal{E}(t)-\mathcal{E}(\infty)$.

This work is preliminary to the study of the stationary driven situation in the presence of a finite force, which will be the subject of a forthcoming publication [11], and where the velocity-force characteristics, and the cross-over between linear and non-linear response will be exposed.

2 Out-of-equilibrium dynamics in the mean field limit

We introduce in this section the mean field dynamical equations and discuss the low temperature, aging solution in the absence of force.

Let $\mathbf{x}(t)$ be the position of the particle, obeying Langevin dynamics:

$$\dot{\mathbf{x}}(t) = -\boldsymbol{\nabla} V(\mathbf{x}(t)) + \mathcal{F} + \boldsymbol{\zeta}(t), \tag{1}$$

where $V(\mathbf{x})$, $\mathcal{F}$, $\boldsymbol{\zeta}(t)$ stand respectively for the random potential, the external force, the Langevin thermal noise $\boldsymbol{\zeta}(t)$ at temperature T (with a friction coefficient equal to 1). The quantities $\mathbf{x}, \boldsymbol{\nabla}, \mathcal{F}, \boldsymbol{\zeta}$ are N-dimensional vectors. Three sub-cases of the dynamics defined by (1) are of interest: 1/ the "isolated" dynamics, without force: $\mathcal{F}=0$; 2/ the driven relaxational dynamics, which is the zero temperature limit of (1): $\mathcal{F}\neq 0$ and $T\to 0$; 3/ the "isolated" relaxational dynamics: $\mathcal{F}=0,\ T\to 0$.

The potential $V(\mathbf{x})$ is a quenched disorder, drawn from a Gaussian distribution. We use an over-line $\overline{\cdot}$ for the average over the quenched disorder, and brackets $\langle\cdot\rangle$ for the average over the thermal noise (if any) ζ. We suppose that the motion starts at $t=0$ and $\mathbf{x}(t=0)=0$. After averaging over the quenched disorder, this choice amounts to starting with a random, "infinite temperature" distribution of initial positions. We expect the process (1) to be self-averaging with respect to $V(\mathbf{x})$ in the infinite dimensional limit. One introduces the correlator $f(y)$ of the Gaussian disorder, explicitly dependent on the dimension N of the configuration space $\{\mathbf{x}\}$.

$$\overline{V(\mathbf{x})\cdot V(\mathbf{x}')} = N f\left(\frac{\|\mathbf{x}-\mathbf{x}'\|^2}{N}\right);\ \overline{V(\mathbf{x})}=0. \tag{2}$$

This form ensures a meaningful $N\to\infty$ limit, in which each coordinate $\mathbf{x}_i(t)$, or gradient component $\partial_i V(\mathbf{x})$, remains of order 1, while the norms $\|\mathbf{x}(t)\|$, $\|\boldsymbol{\nabla} V\|$ scale like $N^{1/2}$. As a consequence, the external force must scale like ($\mathbf{e}_1$ being a unit vector):

$$\mathcal{F} = N^{1/2}\, F\, \mathbf{e}_1. \tag{3}$$

One expects a displacement $\overline{\langle\, \mathbf{x}(t)\,\rangle} = N^{1/2}\, u(t)\, \mathbf{e}_1$, and possibly a mean velocity $\overline{\langle\, \mathrm{d}\mathbf{x}(t)/\mathrm{d}t\,\rangle} = N^{1/2}\, v\, \mathbf{e}_1$. From now onwards, we arrange that $\mathbf{e}_1$ coincides with the first coordinate axis $i=1$.

In what follows, we restrict ourselves to the exponentially correlated potential:

$$f(y) = \exp(-y). \tag{4}$$

This is a special case of short range correlated random potentials, characterized by $\lim_{y\to\infty} f(y) < \infty$. The average difference $\overline{[V(\mathbf{x})-V(\mathbf{x}')]^2}$ is bounded when $\|\mathbf{x}-\mathbf{x}'\|$ grows, and this ensures the existence of a normal diffusion regime at high enough temperatures. Another common choice is the power-law correlator: $f(y)=(1+y)^{(1-\gamma)/2}$; $\gamma>1$ [8–10]. The choice (4) is also equivalent to $f(y)=U_{\mathrm{p}}^2\exp(-y/\xi^2)$, with a pinning energy U_{p} and correlation length ξ set to 1, thanks to a simple rescaling, without loss of generality.

The Langevin dynamics is handled with a Martin-Siggia-Rose (MSR)-like functional integral, convenient for averaging over the quenched disorder [12]. All the details about the saddle-point equations as $N\to\infty$, are given in reference [13] and the resulting action written in Appendix A. The crucial point is that the limit $N\to\infty$ is taken first, before any other limit $T\to 0$ or $t\to\infty$. As a result, we obtain a general effective quadratic action $S[x_j(t), \mathrm{i}\tilde{x}_j(t)]$, involving the original field $x_j(t)$, and the MSR auxiliary field $\mathrm{i}\tilde{x}_j(t)$. Three among the four following correlation functions appear explicitly in the action $S[x_j(t), \mathrm{i}\tilde{x}_j(t)]$:

$$u(t) = N^{-1/2}\ \overline{\langle\, x_1(t)\,\rangle}; \tag{5}$$

$$r(t,t') = N^{-1}\sum_{j=1}^{N} \overline{\langle\, x_j(t)\, \mathrm{i}\tilde{x}_j(t')\,\rangle}; \tag{6}$$

$$b(t,t') = N^{-1}\sum_{j=2}^{N} \overline{\langle\, (x_j(t)-x_j(t'))^2\,\rangle}; \tag{7}$$

$$\begin{aligned} d(t,t') &= N^{-1}\sum_{j=1}^{N} \overline{\langle\, (x_j(t)-x_j(t'))^2\,\rangle}; \\ &= b(t,t') + [u(t)-u(t')]^2. \end{aligned} \tag{8}$$

These are the displacement $u(t)$, the response function $r(t,t')$, and the correlation functions $b(t,t')$ and $d(t,t')$.

The "Dyson equations" for r, b, d, u reduce to a closed system of coupled integrodifferential equations. For $t \geq t'$ one has to solve:

$$\partial_t r(t,t') = \delta(t-t') - \int_0^t \mathrm{d}s\ 4f''(d(t,s))\ r(t,s)\ [r(t,t') - r(s,t')]; \quad (9)$$

$$\partial_t b(t,t') = 2T - \int_0^t \mathrm{d}s\ 4f'(d(t,s))\ [r(t,s) - r(t',s)] - \int_0^t \mathrm{d}s\ 4f''(d(t,s))\ r(t,s)[b(t,s) + b(t,t') - b(s,t')]; \quad (10)$$

$$\partial_t u(t) = F - \int_0^t \mathrm{d}s\ 4f''(d(t,s))\ r(t,s)\,[u(t) - u(s)]. \quad (11)$$

The equations (9–11) are original ones, and allow for a non uniform displacement $u(t)$. The aging, isolated situation is recovered when setting $u(t) = F = 0$, and $d(t,t') = b(t,t')$ in the above system [8,9]. The stationary limit, investigated by Horner [10] amounts to writing $r(t,t') = R(t-t')$, $b(t,t') = B(|t-t'|)$, $u(t) = vt$, and to rejecting the lower bound of the time integrals $\int \mathrm{d}t\ \mathrm{d}s$ to $-\infty$.

Three relevant observables: the energy $\mathcal{E}(t)$, the curvature $\mathcal{M}(t)$ and the pinning force $F_{\mathrm{p}}(t)$, can be expressed with these correlation functions.

$$\mathcal{E}(t) = N^{-1}\ \overline{\langle\, V(\mathbf{x}(t))\,\rangle}, = \int_0^t \mathrm{d}s\ 2f'(d(t,s))\ r(t,s); \quad (12)$$

$$\mathcal{M}(t) = N^{-1} \sum_{j=1}^{N} \overline{\langle\, \partial_{jj}^2 V(\mathbf{x}(t))\,\rangle}, = \int_0^t \mathrm{d}s\ 4f''(d(t,s))\ r(t,s); \quad (13)$$

$$F_{\mathrm{p}}(t) = N^{-1/2}\ \overline{\langle\, -\partial_1 V(\mathbf{x}(t))\,\rangle}, = -\int_0^t \mathrm{d}s\, 4f''(d(t,s))\, r(t,s)\,[u(t) - u(s)]. \quad (14)$$

The pinning force is such that $\overline{\langle\, \mathrm{d}\mathbf{x}(t)/\mathrm{d}t\,\rangle} = \mathcal{F}_{\mathrm{p}}(t) + \mathcal{F}$ with $\mathcal{F}_{\mathrm{p}}(t) = N^{1/2}\, F_{\mathrm{p}}(t)\, \mathbf{e}_1$. The pinning force F_{p} and the driving force F have opposite signs.

A proper study of the mean field equilibrium phase diagram requires an extra quadratic confinement potential $\mu \mathbf{x}^2/2$. This ensures the existence of a true thermal equilibrium in the high temperature phase, while all correlation functions reach their asymptotic values exponentially fast. Then, a transition line $T_{\mathrm{d}}(\mu)$, called dynamical temperature, separates the high temperature ergodic phase, from the low temperature, aging and non-ergodic phase [8,13].

At high temperature, the system reaches a true stationary state, and the dynamics is time-translationally invariant (TTI), *i.e* the two times correlation functions depend only on the difference $t-t'$, while the one time expectation values are constant. In this stationary situation, it is convenient to introduce the TTI correlation functions $B(t-t') = \lim_{t,t'\to\infty} b(t,t')|_{t-t' \text{ finite}}$; $R(t-t') = \lim_{t,t'\to\infty} r(t,t')|_{t-t' \text{ finite}}$. The fluctuation-dissipation theorem (FDT) holds and reads:

$$\mathrm{d}B(t)/\mathrm{d}t = 2T\, R(t). \quad (15)$$

As a consequence, the equal-time correlation functions coincide with their thermodynamical (canonical ensemble) counterparts. Provided the contribution from the harmonic potential has been subtracted off, the energy $\mathcal{E}(t)$ behaves smoothly as μ tends to 0. When μ exactly equals 0, the system cannot be at equilibrium, and instead, one expects a long time behaviour corresponding to a normal diffusion situation, with finite diffusivity $D = \lim_{t\to\infty} \langle\, \mathbf{x}^2(t)\,\rangle/(2Nt)$, finite mobility $\eta^{-1} = \lim_{t\to\infty} u(t)/(Ft)$, and the Einstein relation $D = T\eta^{-1}$.

Kinzelbach and Horner described the dynamics in the stationary, high temperature phase [13]. They found that these correlation functions behave in the same way as those of the well known mode-coupling theories for supercooled liquids, as expected on general grounds [14,16]. The non-linearities of the self-consistent equations cause a dramatic slowing down of the dynamics as T_{d} is approached from above, leading to a sharp transition at $T = T_{\mathrm{d}}$.

For instance, the function $B(t)$, after a fast increase at short times $t \sim 1$, has a long plateau near a characteristic value $B(t \sim t_f) \simeq q$, before eventually reaching its asymptotic, long time regime $B(t) = \hat{B}(t/t_b)$. Both t_f and t_b diverge like power laws of the difference $|T - T_{\mathrm{d}}|$ [13].

The low temperature region, however, corresponds to an out-of-equilibrium situation. In the absence of external force, this is made clear by the loss of both time-translational invariance (TTI) and the fluctuation-dissipation theorem (FDT). The two time correlation functions cannot be reduced any longer to functions of the time difference $t-t'$, and there is a domain in the (t,t') plane, where the system ages [8,9].

The addition of a weak, constant external force leads to a somewhat different picture. As proposed by Horner, the system is expected to reach a stationary state (TTI), but the FDT remains definitively lost [10]. It turns out, however, (*cf.* next section), that when the force is switched on at $t = 0$, there is a finite time interval where the dynamics can be successfully described as a linear perturbation around the isolated, aging regime. The extent of this linear response regime is inversely related to the magnitude of the force.

A comprehensive account of the aging dynamics of the isolated particle can be found in [9]. The fluctuation-dissipation theorem is violated and must be replaced by:

$$X(t,t')\partial_{t'} b(t,t') = r(t,t'). \quad (16)$$

In the time sector ($t-t'$ finite; $t' \to \infty$) of the (t,t') plane, the behaviour is very similar to the one observed just above T_{d}, and the value of $X(t,t')$ is very close to its equilibrium value $-1/(2T)$. When the time separation $t-t'$ is no longer small compared with a characteristic time $t_f(t')$, still to be determined, $X(t,t')$ departs from its equilibrium value, decreasing its magnitude $|X|$.

The analytical solution of (9–11) has, so far, only been found in the asymptotic limit $t, t' \to \infty$, by dropping sub-leading terms presumably of order $1/t, 1/t'$. The crucial observation is that, in this limit, it is possible to parametrize the dynamics with the help of the correlation function $b(t,t')$ of the system. This implies that $X(t,t')$ becomes a one variable function $X[b(t,t')]$, and it turns out that all short range correlated models can be solved thanks to the ansatz [9,17]:

$$\begin{aligned} b(t,t') < q \ &\Rightarrow X[b] = -1/2T; \\ b(t,t') > q \ &\Rightarrow X[b] = \chi. \end{aligned} \tag{17}$$

This extension of the FDT is called the quasi fluctuation-dissipation theorem (QFDT). In this paper, we use instead the function $\overline{T}(t,t') = -1/(2X(t,t'))$. In the aging regime, the effective temperature $\overline{T} = -1/(2\chi)$ is always higher than the thermostat temperature T, and remains finite as $T \to 0$. The meaning of these "two or many temperatures systems" is discussed in [18].

In the case we are interested in, *i.e.* no confinement and correlator $f(y) = \exp(-y)$, χ and q are for any temperature $T < T_{\rm d}$, solutions of [9]:

$$\begin{cases} T = q\sqrt{f''(q)} = \ q\ \mathrm{e}^{-q/2}; \\ \chi = \ \frac{\sqrt{f''(q)}}{2f'(q)} \ = -\mathrm{e}^{q/2}/2; \end{cases} \tag{18}$$

and in the low temperature limit:

$$\begin{cases} q \simeq \quad T + T^2/2 \ldots ; \\ \chi \simeq -\left(\frac{1}{2} + \frac{T}{4} + \frac{3T^2}{16} \ldots\right). \end{cases} \tag{19}$$

In the same way, given a triplet $t_1 < t_2 < t_3$, in the time domain $(t_1, t_2, t_3) \to \infty$ and t_1/t_2, t_2/t_3 finite, $b(t_3, t_2)$ is uniquely determined by the knowledge of $b(t_2, t_1)$ and $b(t_3, t_1)$. Again, the explicit dependence can be carried out exactly when the correlator is exponential. The result is [9]:

$$b(t_3,t_2) - q = b(t_3,t_1) - q - [b(t_2,t_1) - q]. \tag{20}$$

A well known shortcoming of this approach, is that any reference to the original times t, t' is definitively lost. The asymptotic solution cannot distinguish between $b(t,t')$ and $b(h(t), h(t'))$ where $t \mapsto h(t)$ is any reparametrization of the time variable. As a by-product, the previous analysis predicts only the most general form of the solution, in the aging regime $t/t' \sim 1$:

$$b(t,t') = \tilde{B}\left[\ln\left(\frac{h(t)}{h(t')}\right)\right] + q. \tag{21}$$

For exponentially correlated potentials, the master function is known [9] and without loss of generality:

$$b(t,t') = \ln(h(t)) - \ln(h(t')) + q. \tag{22}$$

In [9] the conjecture $h(t) = t^\delta$ is made, which is compatible with the results found below. In what follows, we will refer to this solution as the time-reparametrization invariant (TRI) solution.

At the beginning of the aging regime, for t and t' such that $(t-t')/t'$ is finite but small compared to 1, the scaling form (21), reads:

$$b(t,t') = \tilde{B}\Big((t-t')t_b^{-1}(t') + \ldots\Big) + q. \tag{23}$$

Here, $t_b(t')$ is the characteristic time of the aging regime, defined by $t_b(t') = h(t')/h'(t')$. This is the typical time required by the particle for diffusing over a distance $b(t,t') - q \sim 1$. Conversely, if one knows $t_b(t')$ for all t', one knows $h(t')$. Non exponential correlators have a non analytic scaling function $\tilde{B}(m)$ around $m = 0$ and the r.h.s of (23) is singular in $t - t'$ [9,17].

The time-reparametrization invariant solution describes a situation where the time scales for the FDT regime ($t_0 = 1$) and for the aging regime ($t_b(t')$) are well separated (*i.e.* $t_b(t') \gg 1$), which necessarily implies $t, t' \to \infty$. In particular, the TRI solution does not say how the parameter $\overline{T}$ goes from its FDT value ($b(t,t') < q$) to its QFDT value ($b(t,t') > q$). One defines for this purpose the new time scale $t_f(t)$, such that, for instance, $\overline{T}(t, t - t_f(t))$ takes a given value between T and $-1/(2\chi)$. We shall see below that the two time scales, t_f and t_b, are distinct, and $t_f(t)$ is much smaller than $t_b(t)$ in the large time limit.

3 The numerical integration of the mean field equations

The mean field equations, with F and $u(t)$ equal to zero, were first numerically integrated by Franz and Mézard [8]. This finite difference scheme appears surprisingly robust as the time step h is increased up to values as large as 0.3. The authors of [8] reached $t \sim 1000$ in their longest run. Our investigations showed that the quality of our solutions gets worst when h in increased above 0.2, and we present results up to $t \sim 400$. The numerical method outlined in [19] seems a promising way to improve the quality of the numerics.

For reasons detailed in the next section, we have only considered the exponential correlator case (4). We set T to 0 in (8) and took the initial value $C(0,0) = 0$. The corresponding results can be divided into three categories.

3.1 Results related to the TRI solution

First, we must check that the quasi fluctuation-dissipation relation (17) is true by plotting the integrated response *versus* the correlation function, on Figure 1. The observed value of χ is close to 0.46, while the predicted value is 1/2. The TRI solution also predicts $q \simeq 0$ and $\lim_{t\to\infty} b(t,0) = \infty$ in the absence of confinement. The measured asymptotic energy $\mathcal{E}(\infty)$ and mean curvature $\mathcal{M}(\infty)$ are in excellent agreement with the predicted values -2 and $+4$ respectively.

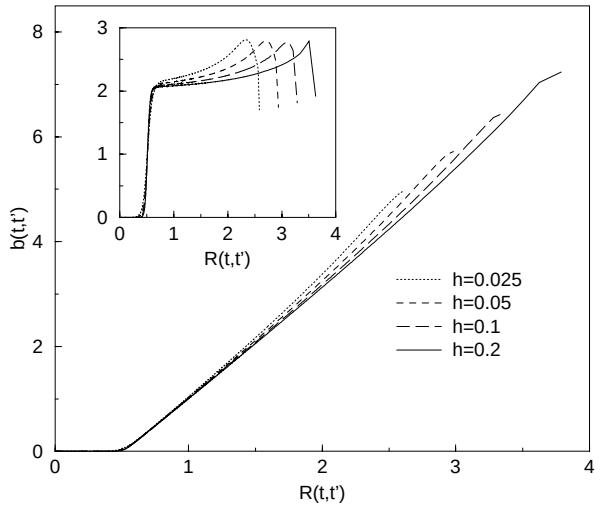

Fig. 1. Parametric plot of the integrated response $b(t,t')$ *vs.* $\mathcal{R}(t,t') = \int_{t'}^{t} \mathrm{d}s\ r(t,s)$ at zero temperature, for time steps $h = 0.025, 0.05, 0.1, 0.2$. The horizontal part corresponds to the short time regime, with $T \to 0$. Then, the aging regime is the straight line with a slope $X^{-1} \simeq 0.21$, to be compared with the theoretical value $1/X_{\mathrm{QFD}} = 2$. The inset shows the derivative $X^{-1}(b) = \mathrm{d}b/\mathrm{d}\mathcal{R}$, stepping from 0 to 2.1.

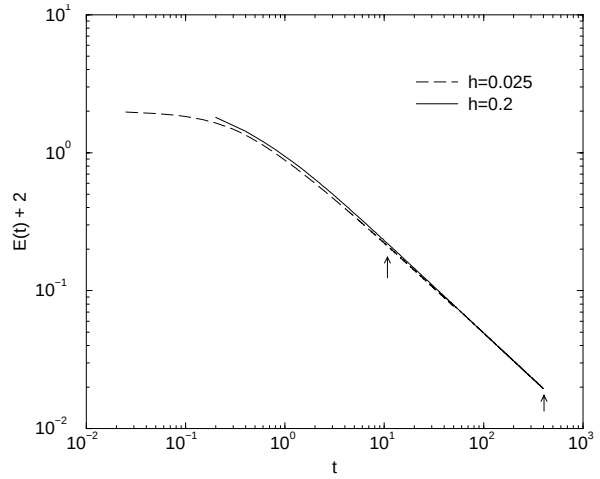

Fig. 2. Dynamical energy $\mathcal{E}(t) + 2$ *vs.* time, in log-log coordinate, for $h = 0.025$ and $h = 0.2$. The power-law decay is unambiguous, and a fit to $\kappa = 0.67$ has been done between the two vertical arrows.

3.2 Beyond the TRI solution, without external force

This includes, for instance, the power law decay of the energy $\mathcal{E}(t) = -2 + c_1\, t^{-\kappa}$. The exponent κ is determined by plotting $\log(2+\mathcal{E}(t))$ *versus* $\log(t)$, and also by computing directly the logarithmic derivative, as shown in Figures 2 and 3. The exponent κ lies between 0.66 and 0.67 and our best estimate is $c_1 = 1.08$.

Also concerned are the characteristic times of the aging regime, and the precise nature of the cross-over from equilibrium to quasi-equilibrium fluctuation-dissipation theorem. We are interested here in finding the characteristic

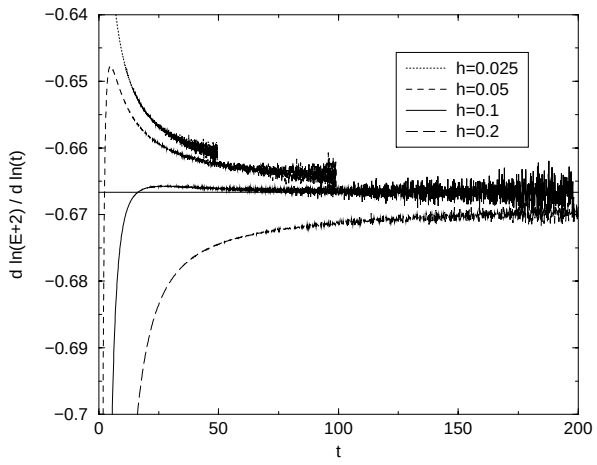

Fig. 3. Logarithmic derivative $-\kappa$ of the energy $\mathcal{E}(t) + 2$, for $h = 0.025, 0.05, 0.1, 0.2$. The curve is noisy as $\mathcal{E}(t) \to -2$. The straight line stands for $\kappa = 2/3$ which we believe to be its exact value. Curves for $h = 0.025, 0.05$ seems to tend to $2/3$ from above, while $h = 0.2$ seems to tend to $2/3$ from below. $\kappa \simeq 2/3$ is well realised for $h = 1$.

time $t_f(t)$ as a function of t, defined by:

$$\int_{t-t_f}^{t} \mathrm{d}s\ 2f'(b(t,s))\ r(t,s) = -1, \tag{24}$$

or alternatively:

$$\int_{t-t'_f}^{t} \mathrm{d}s\ r(t,s) = -\frac{1}{2f'(0)} = \frac{1}{2}\cdot \tag{25}$$

Equation (24) means that the contribution from the quasi-equilibrium regime to the energy is equal to -1. The value t_f which solves (24) separates the equilibrium regime ($b(t,s) < b(t,t-t_f)$) from the aging one ($b(t,s) > b(t,t-t_f)$). The equivalence between (24) and (25) is a straightforward consequence of (17) and (19).

One generalises (25) in:

$$\int_{t-t_a}^{t} \mathrm{d}s\ r(t,s) = a, \tag{26}$$

For $a < 1/2$, t_a must tend to a constant as $t \to \infty$, while for $a > 1/2$, the asymptotic scaling (21) predicts:

$$\begin{aligned} a - 1/2 &= -\chi\ \tilde{B}\left[\ln\left(\frac{h(t)}{h(t-t_a)}\right)\right]; \\ &\simeq -\chi\ \tilde{B}(t_a/t_b), \end{aligned} \tag{27}$$

where terms $(t_a/t_b)^2$ have been neglected in the last expression, and $t_b = h(t)/h'(t)$. If $a - 1/2$ is small enough, t_a is simply proportional to t_b. Moreover, if $h(t)$ is indeed t^δ, then $a - 1/2 = -\chi\ \tilde{B}_1((1 - t_a/t_b)^{-\delta})$, and t_a/t_b is strictly constant. Our Figure 4 shows a plot of t_f, $t_{a=0.55}$, and $t_{a=0.45}$. The characteristic time scale t_f tends asymptotically towards a power law $c_2 t^\alpha$, with $c_2 \simeq 0.51$ and $\alpha \simeq 0.64$ (according to our best estimate).

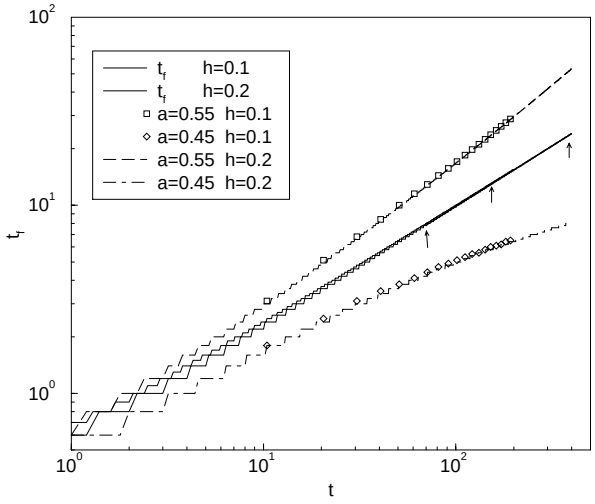

Fig. 4. The characteristic times $t_f(t) \propto t^\alpha$ and $t_a(t)$, $a = 0.55$ and $a = 0.45$ determined from equations (24–26). Results are shown for the time steps $h = 0.1$ and $h = 0.2$, and the finiteness of h is visible at small t. A numerical estimate of α is 0.64 between the first and last vertical arrows. The exponent of $t_{a=0.55}$ is close to 0.93 while we expect 1, and $t_{a=0.45}$ should saturate to a constant.

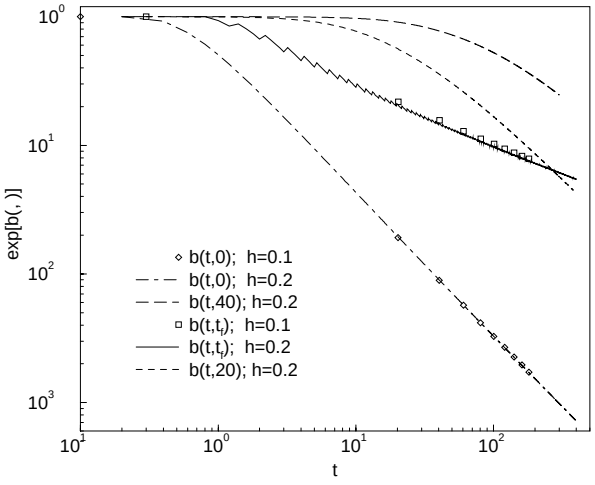

Fig. 5. The functions $\exp[-b(t,0)]$, $\exp[-b(t,t-t_f(t))]$ *vs.* t, for $h = 0.2$ and $h = 0.1$, in logarithmic coordinates. The functions $\exp[-b(t,20)]$ *vs.* $(t-20)$ and $\exp[-b(t,40)]$ *vs.* $(t-40)$. Here, 20 and 40 are waiting times. The behaviour of $b(t,0)$ and $b(t,t-t_f(t))$ is doubtless logarithmic. The slopes of $\exp[-b(t,0)]$, $\exp[-b(t,t-t_f(t))]$, in this figure, are respectively -1.10 and -0.42. According to the predictions of [9], $\exp(-b(t,t'))$ tends to $h(t) - h(t')$ for $t, t' \gg 1$; t/t' finite. The curves $\exp[-b(t,20)]$ and $\exp[-b(t,40)]$ tend to imitate $\exp[-b(t,0)]$, with a delay.

The correlation function is found to grow logarithmically with t, and $f(b(t,t')) = \exp(-b(t,t'))$ behaves as a power law of t. Figure 5 presents $\exp(-b(t,0))$ and $\exp(-b(t,t'))$ for a fixed t'. A power law decay $t^{-\delta}$ of $\exp(-b(t,0))$ is likely, while $\exp(-b(t,t'))$ has not yet reached its asymptotic regime, but could join the same $t^{-\delta}$ behaviour.

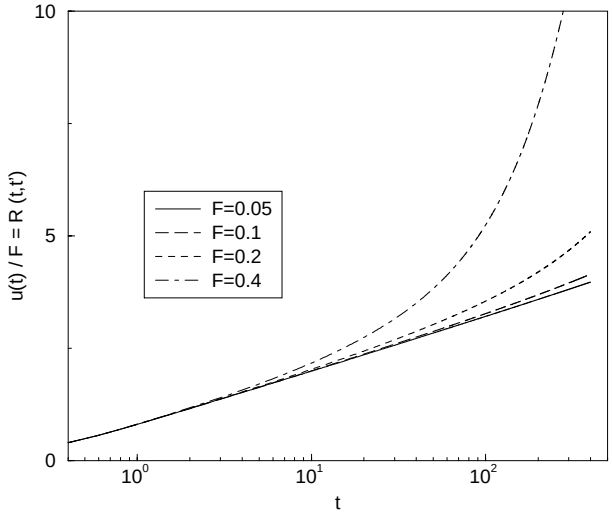

Fig. 6. A test of the linear response of the displacement $u(t)$. We plot $u(t)/F$, as a function of $\ln(t)$, for $F = 0.05, 0.1, 0.2$ and 0.4; $h = 0.2$. As $F \to 0$, the curves are indistinguishable from the integrated response $\mathcal{R}(t)$. A departure from the straight line signals the breakdown of the linear response, as the particle acquires a finite velocity, dependent (non-linearly) on the force. The suggested behaviour of $u(t)$ is thus: $u(t) = F(c_3 + c_4 \ln(t))$.

From the asymptotic form (21, 22) we note that $\exp(-b(t,t')) \simeq h(t')/h(t)$; $t, t' \to \infty$; t/t' finite, and our figure is consistent with $h(t) = t^\delta$, $\delta \simeq 1.10$. Also shown is $\exp(-b(t, t-t_f)) = t^{-\gamma}$, $\gamma \simeq 0.42$. Expanding $\exp(-b(t,t_f))$ as $(t/t_f)^{-\delta}$, and using $t_f \sim t^\alpha$, one finds the relation $\gamma = \delta(1-\alpha)$ between exponents. The agreement between $\delta(1-\alpha) = 0.39$ and $\gamma \simeq 0.42$ is acceptable.

3.3 The linear displacement regime, in the presence of a driving force

A small force F is applied and the displacement $u(t)$ monitored. The linear response implies that $u(t)$ must be proportional to F, and it is indeed the case for time intervals not too large. Figure 6 presents $u(t)/F$ for decreasing values of F. The curve $F = 0.05$ is virtually indistinguishable from the integrated response $\mathcal{R}(t) = \int_0^t r(t,s)\mathrm{d}s$, and this shows that $\lim_{F\to 0} u_F(t)/F = \mathcal{R}(t)$, *i.e.* the expected linear response behaviour. The other curves depart from the integrated response after a time t_F decreasing with F. The linear response only holds during a finite time interval $0 < t \leq t_F$. What happens later is the onset of a stationary state, with a well defined velocity v and a non-linear dependence on the force, as advocated by Horner [10]. A study of this regime is left to a separate publication [11].

In the linear response regime, Figure 6 is compatible with:

$$u(t) = F(c_3 + c_4 \ln(t)), \tag{28}$$

$c_3 \simeq 0.71$ and $c_4 = 0.54$.

4 The geometrical approach

In this section, we transpose to the particle in a random potential a method which was successfully applied to the spherical p-spin model, namely the geometrical analysis of Kurchan and Laloux [7]. We first present this approach, and then compute the limiting value of the dynamical energy from purely geometrical considerations, provided the random potential has exponential correlations $f(y) = \exp(-y)$.

The p-spin model starts aging below a critical temperature T_d [2], and has a thermodynamical glassy transition at $T_\mathrm{s} < T_\mathrm{d}$ [23]. These two transitions are understood thanks to the concept of free-energy landscape, which accounts for many features of both thermodynamics [24–26] and dynamics [3,27].

The configurations space of the p-spin model can be analysed by means of a Thouless-Anderson-Palmer (TAP) free-energy $\Phi(m_i)$ of the magnetization m_i ($i = 1 \dots N$). At low temperature, the function Φ develops many extrema $m_i^{(\alpha)}$, the TAP solutions α. Those extrema which are minima, *i.e.* the second derivative matrix $\partial^2\Phi/\partial m_i \partial m_j$ is positive definite, are metastable states, as they are separated from each others by extensive free-energy barriers. In the thermodynamic limit, a particular realization of the system, prepared in a given metastable state α remains for ever in this state.

The stability of a metastable state is related to the lowest eigenvalue λ_min of $\mathrm{Spec}(\partial^2\Phi/\partial m_i \partial m_j)$, spectrum of the Hessian matrix. λ_min turns out to be a monotonically decreasing function of the free energy $\Phi(m_i^{(\alpha)})$ of the state. This defines the free-energy Φ_d of the marginal states as $\lambda_\mathrm{min} = 0$ for $\Phi = \Phi_\mathrm{d}$. Magnetizations such that $\Phi(m_i) \geq \Phi_\mathrm{d}$ correspond to regions of negative curvature which do not contribute to the thermodynamics but play a role in the dynamics [20].

The glassy dynamics of the p-spin model is observed when the stable metastable states $\Phi^{(\alpha)} < \Phi_\mathrm{d}$ are populated, or equivalently, when the canonical Boltzmann measure is split into its metastable components α. At a temperature lower than T_d, thermal equilibration requires the system to explore all the relevant metastable states $\Phi < \Phi_\mathrm{d}$. Such an equilibration is impossible as going from one metastable state to the next requires a jump over an infinite barrier. What happens instead to a system quenched from high temperature, to $T < T_\mathrm{d}$, is the onset of aging. The configuration of the system evolves more and more slowly in the region where $\Phi(m_i) \simeq \Phi_\mathrm{d}$, *i.e.* around the marginal states.

The zero temperature relaxational dynamics is simpler because the free energy reduces to the Hamiltonian H of the spins s_i. At variance with the finite temperature case, the regions with negative curvature of H are now well defined. Taking the limit $T \to 0$ in the mean-field equations does not lead to any singular behaviour. This somewhat counter-intuitive property is the consequence of sending $N \to \infty$ first, while keeping finite the times t and t'. The dynamics is a pure gradient descent, but remains non-trivial.

In order to perform a geometrical analysis of this relaxational dynamics, it is necessary to start with a large but finite dimension N. Then, the relaxational process takes place until the particle falls into a local minimum of the Hamiltonian $H(s_i)$, and (at $T = 0$) remains stuck there forever. According to the description advocated in [7], a system starting from a random configuration $\{s_i(0)\}$, explores regions with smaller and smaller gradient $\|\boldsymbol{\nabla} H(s_i)\|$, and a decreasing number of negative eigenvalues in the spectrum of $\mathcal{H}_{ij}$, Hessian of $H(s_i)$. The typical time t_N^I for reaching regions where $\mathcal{H}_{ij}$ has only I negative eigenvalues, diverges as N is sent to ∞, keeping I finite [7]. As a consequence, in the limit $N \to \infty$, the system is unable to reach a local minima within a finite time, or even a saddle between two minima, and the difference $\mathcal{E} - \mathcal{E}_\mathrm{d}$ remains positive.

To what extent does the above picture correctly describe a particle in a random potential ? There is no obvious explicit form for the free energy function $\Phi(\langle\, \mathbf{x}\,\rangle)$ of the mean position $\langle\, \mathbf{x}\,\rangle$ of the particle, and much less is known about the properties of the corresponding metastable states. Nonetheless, we expect that the basic mechanism for the dynamical transition remains the same as for the spherical p-spin model, *i.e.* a slow relaxation towards a region of marginal states, $\lambda_\mathrm{min} \sim 0$. When considering the zero temperature limit, the dynamics reduces to a gradient descent $\dot{\mathbf{x}}(t) = -\boldsymbol{\nabla} V(\mathbf{x}(t))$. The metastable states now correspond to local minima of the potential $V(\mathbf{x})$, and their stability will depend on the spectrum of the Hessian $\mathcal{H}_{ij} = \partial_{ij}^2 V(\mathbf{x})$, where ∂_i means $\partial/\partial x_i$ and $\partial_{ij}^2 = \partial^2/\partial x_i \partial x_j$.

The purpose of the geometrical approach is to relate the values provided by the more formal field-theoretical approach, to some basic properties of the potential $V(\mathbf{x})$. For instance, one must be able to compute the asymptotic values of the energy $\mathcal{E}(t)$, curvature $\mathcal{M}(t)$, and the "plateau value" $\lim_{T\to 0} q/T$ of the correlation function. This is the first step, already outlined in [7]. In the following sections, we attempt to understand, using geometrical arguments, more subtle properties of the aging behaviour, beyond the time reparametrization invariant solution.

4.1 Characterization of the energy landscape

The central point is to relate the relaxation dynamics to the energy landscape. Because of the close connection between dynamics and the "marginality" of the landscape, we propose to consider the spatial average:

$$\langle\, \mathrm{Spec}(\mathcal{H})\,\rangle = \overline{\frac{\int_\mathcal{D} \mathrm{d}\mathbf{x}\ \delta(V(\mathbf{x}) - V_0)\ \mathrm{Spec}(\mathcal{H})(\mathbf{x})}{\int_\mathcal{D} \mathrm{d}\mathbf{x}\ \delta(V(\mathbf{x}) - V_0)}}\,. \qquad (29)$$

Here, $\mathcal{H}$ is the "dynamical matrix", Hessian of the potential energy V, and function of the coordinates $\mathbf{x}_i$. $\mathrm{Spec}(\mathcal{H})$ stands for a characteristic function of the eigenvalues spectrum, *e.g.* the density of states. $\mathcal{D}$ is a bounded domain, eventually becoming infinite.

The expression (29) is reminiscent from the usual instantaneous normal modes (INM) definition introduced

in the context of supercooled liquids dynamics [21], *i.e.* the canonically averaged spectrum of $\mathcal{H}$, ($Z_{\mathcal{D}}$ partition function):

$$\langle\, \mathrm{Spec}(\mathcal{H})\,\rangle = \overline{Z_{\mathcal{D}}^{-1} \int_{\mathcal{D}} \mathrm{d}\mathbf{x}\ (\mathrm{e}^{-\beta V}\, \mathrm{Spec}(\mathcal{H}))}. \tag{30}$$

In the mean field model considered here, the above canonical average is dominated by a temperature dependent saddle-point $V_0 = V(\beta)$, making (30) equivalent to (29).

In the p-spin glass case, the average spectrum of $\mathcal{H}$ has a semi-circular shaped density of states, shifted by an amount, function of V_0 only. The fluctuations of the index of $\mathcal{H}$, given an energy V_0, have been calculated, and are exponentially small with the number of spins N [22].

The expression (29) characterizes the correlations between the energy of a point, and the local curvature around it. In what follows, we use (29) to determine the dynamical energy $\lim_{t\to\infty} \mathcal{E}(t)$, by asking $\mathrm{Spec}(\mathcal{H})$ to be marginal. It is important to notice that we do not refer at all to the value of the gradient $\boldsymbol{\nabla} V(\mathbf{x})$ in expression (29). In particular, the sum over $\mathbf{x}$ is not restricted to the stationary points $\boldsymbol{\nabla} V(\mathbf{x}) = 0$. Thus, it is legitimate to check whether the value of the gradient influences $\mathrm{Spec}(\mathcal{H})$ or not. It could be that regions with both $V(\mathbf{x}) = V_0$ and $\|\boldsymbol{\nabla} V\|^2 < \varepsilon$ (ε arbitrary small positive number), have an averaged spectrum quantitatively different from the unrestricted case (29). As the magnitude of $\boldsymbol{\nabla} V(\mathbf{x}(t))$ tends to zero for large times, this would affect the value of the dynamical energy.

A recent work on a realistic potential (binary mixture of "Lennard-Jones" interacting species) showed evidence of such a phenomenon, as the average index of the stationary points (the so-called saddles) differs from the unrestricted (INM like) average, at the same potential energy [28]. However, at the mean field level, we failed to establish any relation between the magnitude of the gradient $\boldsymbol{\nabla} V(\mathbf{x})$ and the Hessian $\mathcal{H}(\mathbf{x})$, which look uncorrelated. This is why we consider the expression (29), computed in the next paragraph, as a suitable characterization of the energy landscape.

4.2 The spectrum of H

The averaged spectrum $\langle\, \mathrm{Spec}(\mathcal{H})\,\rangle$, as defined by (29), is a natural quantity to consider when looking at the zero temperature relaxational dynamics of our mean field model. We found that, as far as exponentially correlated potentials are concerned, $\mathrm{Spec}(\mathcal{H})$ is, at the leading order, a non fluctuating quantity determined solely by V_0. More precisely, $\mathrm{Spec}(\mathcal{H})$ is a semi-circular distribution of radius Λ, centred around $\mathcal{D}$.

$$\Lambda = 4\sqrt{f''(0)}; \tag{31}$$

$$\mathcal{D} = \frac{2f'(0)}{f(0)} \frac{V_0}{N}. \tag{32}$$

Let us outline our demonstration. We consider first the ($\mathbf{r}$ independent) "annealed average".

$$\overline{\delta(V(\mathbf{r}) - V_0)\ \mathrm{Spec}(\mathcal{H})(\mathbf{r})}. \tag{33}$$

In order to compute (33), it is enough to enumerate the correlations of $V(\mathbf{r}), \partial_{ij} V(\mathbf{r})$, where $\mathbf{r}$ is an arbitrary point. All the $\partial_{ij} V(\mathbf{r})$ are independent at the leading order N^{-1}, whereas the $N+1$ remaining variables $V(\mathbf{r}), \partial_{ii} V(\mathbf{r})$ are found to be correlated. One has:

$$\begin{aligned}
N\,\overline{[\partial_{ij} V(\mathbf{r})]^2} &= 4f''(0) + \mathcal{O}(N^{-1});\\
N\,\overline{[\partial_{ii} V(\mathbf{r})]^2} &= 12f''(0) + \mathcal{O}(N^{-1});\\
N\,\overline{\partial_{ii} V(\mathbf{r}) \cdot \partial_{jj} V(\mathbf{r})} &= 4f''(0) + \mathcal{O}(N^{-1});\\
\overline{V(\mathbf{r}) \cdot \partial_{ii} V(\mathbf{r})} &= 2f'(0) + \mathcal{O}(N^{-1});\\
N^{-1}\,\overline{[V(\mathbf{r})]^2} &= f(0) + \mathcal{O}(N^{-1}).
\end{aligned} \tag{34}$$

$\mathcal{H}$ is split into a scalar part $\mathcal{D}\delta_{ij}$ and a fluctuating part $\mathcal{H}'$. The elements of $\mathcal{H}'$ are independent and Gaussian, and its eigenspectrum has, at the leading order, a semi-circular shape of radius $4\sqrt{f''(0)}$ centred around 0. If $N \to \infty$ and $V(\mathbf{r})/N$ finite, then $\mathcal{D}$ is constant, up to fluctuations of order $N^{-1/2}$ (*cf.* Appendix B).

$$\mathcal{D} = \frac{2f'(0)}{f(0)} \frac{V(\mathbf{r})}{N} + \mathcal{O}(N^{-1/2}). \tag{35}$$

The resulting spectrum is the one announced in equations (31, 32).

In order to bridge the gap between (29) and (33), we consider now the two points average:

$$\overline{\delta(V(\mathbf{r}) - V_0)\ \delta(V(\mathbf{r}_1) - V_1)\ \mathrm{Spec}(\mathcal{H})(\mathbf{r})}. \tag{36}$$

The analysis now involves correlations between $V(\mathbf{r})$, $\partial_{ij} V(\mathbf{r})$, $V(\mathbf{r}_1)$, $\partial_{ij} V(\mathbf{r}_1)$. One finds that for a generic correlator $f(y)$, $\mathrm{Spec}(\mathcal{H})(\mathbf{r})$ depends on both $V(\mathbf{r})$ and $V(\mathbf{r}_1)$. However, if $f(y)$ obeys $ff'' - (f')^2 = 0$, with $f(y) = \exp(-y)$ as a particular case, the dependence in $V(\mathbf{r}_1)$ disappears, and the result (32) holds.

Computing

$$\begin{aligned}
&\overline{\delta(V(\mathbf{r}) - V_0)\ \delta(V(\mathbf{r}_1) - V_1) \dots}\\
&\overline{\times \delta(V(\mathbf{r}_n) - V_n) \mathrm{Spec}(\mathcal{H})(\mathbf{r})},
\end{aligned} \tag{37}$$

becomes very difficult as $n \geq 3$, and we were not able to find a close expression for $\mathrm{Spec}(\mathcal{H})(\mathbf{r})$ $(V_0, V_1, \dots, V_n)$. However, if $ff'' - (f')^2 = 0$, again $\mathrm{Spec}(\mathcal{H})(\mathbf{r})$ depends only on V_0, and (32) is valid. This shows that the spectrum of $\mathcal{H}$ is a local quantity, independent of the environment of the particle.

Because $\mathrm{Spec}(\mathcal{H}(\mathbf{r}))$ is a function of $V(\mathbf{r})$ only, we conclude that the average (29) is described by (31, 32) and that the self-averaging property of $\mathrm{Spec}(\mathcal{H})(\mathbf{r})$, and its linear dependence in $V(\mathbf{r})$, which was true for the p-spin model, is still true for exponential correlators. The Appendix B gives further details on the computation of (33) and (36).

4.3 Comparison with the formal approach

Now, we assume that the trajectory $\mathbf{x}(t)$ explores representative regions of the potential (*i.e.* non-exceptional

points), for which the above mentioned results hold. The lowest eigenvalue $-\mathcal{S}$ of the Hessian, defined by (32) becomes a time-dependent function:

$$\mathcal{S}(t) = \Lambda - \frac{2f'(0)}{f(0)}\mathcal{E}(t), \tag{38}$$

leading to the energy dependent (through $\mathcal{S}$) density of eigenvalues of $\mathcal{H}_{ij}$. The number of eigenvalues between $\lambda - \mathcal{S}(t)$ and $\lambda - \mathcal{S}(t) + \mathrm{d}\lambda$ is $\rho(\lambda)\mathrm{d}\lambda$ (time independent).

$$\rho(\lambda) = 2(\pi\Lambda^2)^{-1}\sqrt{\lambda\ (2\Lambda - \lambda)}. \tag{39}$$

The marginality condition, by definition, is $\mathcal{S} \equiv 0$. Equation (38) yields the "geometrical energy", necessary for $\mathcal{H}$ to be marginal:

$$\mathcal{E}_{\mathrm{geom}} = 2\frac{\sqrt{f''(0)}f(0)}{f'(0)}, \tag{40}$$

and the curvature $\mathcal{M}_{\mathrm{geom}}$:

$$\begin{aligned}\mathcal{M}_{\mathrm{geom}} &= \int \mathrm{d}\lambda\lambda\ \rho(\lambda),\\ &= 4\sqrt{f''(0)}.\end{aligned} \tag{41}$$

After a time t long enough, the particle evolves in a marginal region ($\mathcal{S}(t) \simeq 0$) of the potential $V(\mathbf{x})$, with a small gradient $\|\boldsymbol{\nabla} V(\mathbf{x})\|$. At low temperature, the potential may be developed up to the second order by means of local coordinates y_i: $V(\mathbf{y}) = V(0) + \mathbf{y}\cdot\boldsymbol{\nabla}V(0) + \sum_{i=1,N}\lambda_i y_i^2/2$. The plateau value "$q$" of the correlation function $b(t,t')$ is thus given by assuming that each direction of curvature λ_i is thermalized with $\langle\, y_i^2\,\rangle \simeq T/\lambda_i$, and $q = 2N^{-1}\sum_{i=1,N}\langle\, y_i^2\,\rangle$:

$$\begin{aligned}q_{\mathrm{geom}} &= \int_0^{8\sqrt{f''(0)}} \mathrm{d}\lambda \frac{2T}{\lambda}\ \rho(\lambda)|_{S=0},\\ &= \frac{T}{\sqrt{f''(0)}}.\end{aligned} \tag{42}$$

Let us compare now these findings with the dynamical mean-field results, in the zero temperature limit [9].

$$\lim_{t\to\infty}\mathcal{E}(t) = \frac{f'(0)}{\sqrt{f''(0)}} + \frac{f(0)\sqrt{f''(0)}}{f'(0)}, \tag{43}$$

$$\lim_{t\to\infty}\mathcal{M}(t) = 4\sqrt{f''(0)}, \tag{44}$$

$$q = \frac{T}{\sqrt{f''(0)}}. \tag{45}$$

Agreement holds for the curvature and q, whereas the geometrical and dynamical energy differ, unless $f(0)f''(0) = f'(0)^2$. We cannot conclude about the relevance of the geometrical approach for a generic correlator, *e.g.* power law, as (32) probably does not hold in this case. It is also possible in this case that the local environment ($\boldsymbol{\nabla}V\ \ldots$), and not just the potential energy, control the Hessian properties, making the expression (29) irrelevant.

However, the exponentially correlated model turns out to be a very favourable one, for which the geometrical approach gives sensible results. We claim that many features of the zero temperature dynamics of this model (exponents, aging, driving with a force) can be explained with geometrical arguments.

5 The distribution of the gradient's coordinates

In this section, we introduce an orthonormal frame "attached" to the particle, as in the instantaneous normal mode description of liquids [21]. Then, we investigate the statistical properties of the components of $\boldsymbol{\nabla}V(\mathbf{x}(t))$ in this special frame. We find that these components are distributed according to a self-similar form, determined by the value of the exponent κ of the energy decay.

We develop up to the second order the potential around the actual position of the particle $\mathbf{x}(t)$.

$$\begin{aligned}\mathbf{Q}(\mathbf{x}) = V(\mathbf{x}(t)) + \sum_i (\mathbf{x}_i - \mathbf{x}_i(t))\cdot\partial_i V(\mathbf{x}(t))\\ +1/2\sum_{ij}\partial_{ij}V(\mathbf{x}(t))\cdot(\mathbf{x}_i - \mathbf{x}_i(t))\cdot(\mathbf{x}_j - \mathbf{x}_j(t)).\end{aligned} \tag{46}$$

We consider the orthonormal frame of eigendirections $\{\mathbf{e}_{\lambda_i}(t)\}$ which diagonalizes $\mathcal{H}_{ij}(t) = \partial_{ij}^2 V(\mathbf{x}(t))$. λ_i belongs to the – time independent – interval $[0, 2\Lambda]$, so that the corresponding eigenvalue of $\mathbf{Q}$ is just $\lambda_i - \mathcal{S}(t)$.

We follow "adiabatically" the eigenvectors $\{\mathbf{e}_{\lambda_i}(t)\}$ as the particle moves. A mild assumption is that the $\{\mathbf{e}_{\lambda_i}\}$ evolve smoothly, provided the levels λ_i are allowed to freely cross each other. This choice implies that any ordering of the λ_i lasts only for a short period of time. The $\{\mathbf{e}_{\lambda_i}\}$ define a comoving frame, in which the gradient $\boldsymbol{\nabla}V$, or equivalently the velocity, can be projected.

$$\begin{aligned}-\boldsymbol{\nabla}V(\mathbf{x}(t)) &= \sum_i \boldsymbol{\gamma}_i(t)\mathbf{e}_{\lambda_i}(t),\\ &= \dot{\mathbf{x}}(t).\end{aligned} \tag{47}$$

There are reasons to think that the components $\boldsymbol{\gamma}_i(t)$ are randomly and evenly distributed, even in the deterministic zero temperature limit. First, this randomness reflects the average over the initial conditions. Then, as the correlator $\overline{\partial_{ij}^2 V(\mathbf{x})\partial_{ij}^2 V(\mathbf{x}')}$ is exponentially short range correlated, one can suppose that the comoving frame is rotating on itself in a chaotic manner, as it does in the spherical ($p \geq 3$)-spin model [7]. So, during the particle's motion, each component $\boldsymbol{\gamma}_i$ spreads continuously over the $N-1$ others directions.

The sign of the $\boldsymbol{\gamma}_i(t)$ is arbitrary, because of the non uniqueness of the frame, invariant under the reflections $\mathbf{e}_{\lambda_i} \leftrightarrow -\mathbf{e}_{\lambda_i}$. Thus, we consider $\boldsymbol{\gamma}_i^2(t)$ rather than $\boldsymbol{\gamma}_i(t)$. On physical ground, we propose to consider only the smooth quantity $\lceil\boldsymbol{\gamma}_i^2(t)\rfloor$, obtained by a local average over the few $\sqrt{N}$ indices j such that $\lambda_i - N^{-1/2} < \lambda_j < \lambda_i + N^{1/2}$.

This is possible because the mean space between two consecutive λ_i is $\mathcal{O}(N^{-1})$. As N goes to ∞, one expects $\left\lceil \boldsymbol{\gamma}_i^2(t) \right\rfloor$ to become a smooth function of λ_i, varying only on the scale $\delta\lambda \sim 1$ (although, rigorously, the scale of variation could be only $\delta\lambda \sim N^{-1/2}$), making the dependence in the index i irrelevant. The function:

$$g(\lambda_i, t) = \left\lceil \boldsymbol{\gamma}_i^2(t) \right\rfloor, \tag{48}$$

is the distribution of the gradient's coordinates (or equivalently of the instantaneous velocity coordinates) and is a central object in the present study.

In this continuous limit, the two first time derivatives of $\mathcal{E}$ can be expressed with the help of the density $\rho(\lambda)$ and the distribution $g(\lambda, t)$ as:

$$\begin{aligned}\dot{\mathcal{E}}(t) &= -\sum_i \partial_i V(\mathbf{x}(t)) \cdot \partial_i V(\mathbf{x}(t)),\\ &= -\int \mathrm{d}\lambda\ \rho(\lambda)\ g(\lambda, t). \qquad (49)\\ \ddot{\mathcal{E}}(t) &= \sum_{ij} \partial_j V(\mathbf{x}(t)) \cdot \partial_{ij} V(\mathbf{x}(t)) \cdot \partial_i V(\mathbf{x}(t)),\\ &= \int \mathrm{d}\lambda\ \rho(\lambda)\ (\lambda - \mathcal{S}(t))\ g(\lambda, t). \qquad (50)\end{aligned}$$

In [7] was already noticed that, due to the algebraic decay of the energy $\mathcal{E}(t) = -2 + 1.08\, t^{-\kappa}$, the ratio $\ddot{\mathcal{E}}(t)/\dot{\mathcal{E}}(t)$ was $\sim 1/t$. From Section 3, we know that $\mathcal{S}(t) \sim t^{-0.67}$, which implies $\ddot{\mathcal{E}}(t) \ll \mathcal{S}(t) \cdot \dot{\mathcal{E}}(t)$, and thus:

$$\begin{aligned}\int \mathrm{d}\lambda\ \rho(\lambda)\ \lambda g(\lambda, t) &= \ddot{\mathcal{E}}(t) + \mathcal{S}(t) \int \mathrm{d}\lambda\ \rho(\lambda) g(\lambda, t), \qquad (51)\\ &\simeq \mathcal{S}(t) \int \mathrm{d}\lambda\ \rho(\lambda) g(\lambda, t). \qquad (52)\end{aligned}$$

The first moment of $g(\lambda, t)\ \rho(\lambda)$, is proportional to $\mathcal{S}(t)$, suggesting a self-similar scaling form for $g(\lambda, t)$, valid for $t \to \infty$ and $T = 0$ (Fig. 7):

$$g(\lambda, t) = \Gamma(t)\ \hat{G}\left(\frac{\lambda}{\mathcal{S}(t)}\right). \tag{53}$$

The knowledge of the other moments of g would be useful to confirm equation (53), but unfortunately, they are very difficult to compute, and are no more given by the next derivatives of $\mathcal{E}$.

As t increases, only the smallest λ_i are relevant, and the density ρ is well approximated by its $\lambda \sim 0$ equivalent $\pi^{-1}(2/\Lambda)^{3/2}\sqrt{\lambda}$. In this limit, the decrease rate of the energy is, from (49) and (53):

$$\dot{\mathcal{S}}(t) = -\frac{2f'(0)}{f(0)}\dot{\mathcal{E}}(t) \propto -\Gamma(t)\mathcal{S}(t)^{3/2}. \tag{54}$$

The knowledge of the exponent κ of $\mathcal{S}(t) \sim t^{-\kappa}$ (Sect. 3) fixes the prefactor Γ up to a constant, to:

$$\Gamma = \mathcal{S}^{(2-\kappa)/2\kappa}. \tag{55}$$

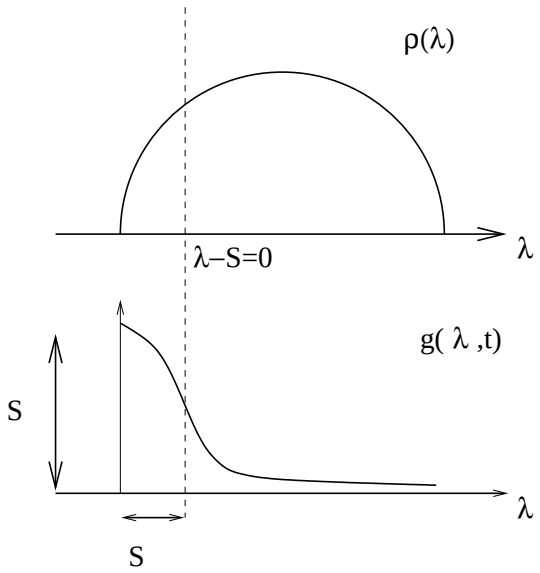

Fig. 7. The density $\rho(\lambda)$ of eigenvalues $\lambda - \mathcal{S}$ (on top). A sketch of the self-similar distribution $g = \mathcal{S}\hat{G}(\lambda/\mathcal{S})$, assuming $\Gamma = \mathcal{S}$ (bottom). The tail of $\hat{G}$ goes to 0 as $\lambda/\mathcal{S} \to \infty$, in the asymptotic limit $\mathcal{S} \to 0$.

Our Section 2 suggests κ is very close to 2/3, which would imply $\Gamma \propto \mathcal{S}$.

The next momentum of $g(\lambda, t)\rho(\lambda)$ provides information on the time correlations of the unit vector $\mathbf{w}(t)$ of the particle's trajectory. On the one hand,

$$\begin{aligned}\Big(\partial_t \boldsymbol{\nabla} V(\mathbf{x}(t))\Big)^2 &= \sum_i \left(\sum_j -\partial_j V(x(t)) \partial_{ij} V(x(t))\right),\\ &\quad \times \left(\sum_k -\partial_k V(x(t)) \partial_{ik} V(x(t))\right),\\ &= \sum_{i,j,k} \partial_j V\, \partial_{ji} V\, \partial_{ik} V\, \partial_k V,\\ &= \int \mathrm{d}\lambda\ \rho(\lambda)\ (\lambda - \mathcal{S}(t))^2\ g(\lambda, t). \qquad (56)\end{aligned}$$

With the scaling form for $g(\lambda, t)$, the right hand side is of order $\Gamma(t)\mathcal{S}(t)^{7/2}$. On the other hand, we perform a decomposition $-\boldsymbol{\nabla} V(\mathbf{x}(t)) = M(t)\ \mathbf{w}(t)$. The norm $M(t)$ equals $(-\dot{\mathcal{E}}(t))^{1/2}$, and $\mathbf{w}(t)$ is the unit vector, tangent to the trajectory. The following equality holds:

$$(\partial_t \boldsymbol{\nabla} V)^2 = (\partial_t M)^2 + M^2 \|\partial_t \mathbf{w}\|^2. \tag{57}$$

This sum is clearly dominated by $M^2\|\partial_t \mathbf{w}\|^2$, with $M^2 \simeq \Gamma\mathcal{S}^{3/2}$. The unitary vector rotates, irrespective of the actual value of $\Gamma(t)$, at a rate $\|\partial_t \mathbf{w}\| \sim \mathcal{S}(t)$. One expects the "director" $\mathbf{w}(t)$ to have changed its orientation after a typical time $\mathcal{S}(t)^{-1}$, which looks like a "persistence time" for the trajectory of the particle. Consequently, the motion of $\mathbf{x}(t)$ crosses over from a "ballistic" regime $\|\mathbf{x}(t + \delta t) - \mathbf{x}(t)\| \sim M^2(\delta t)^2;\ \delta t \ll \mathcal{S}^{-1}$ to a diffusive

regime $\|\mathbf{x}(t+\delta t)-\mathbf{x}(t)\| \sim D\delta t;\ \delta t \gg \mathcal{S}^{-1}$. The existence of a diffusive regime is here inferred by the expansion (21, 23), valid only for exponentially correlated disorder, and by no means generic.

6 A short time, quasi-static approximation

We investigate here the early stage of the fluctuation-dissipation theorem violation, measured by the function $\overline{T}(t,t')$ (*cf.* 17). We propose a model for the short time evolution of $\overline{T}(t,t')$, and show that its predictions are in good agreement with the findings of Section 2.

We approximate locally the potential $V(\mathbf{x})$ around $\mathbf{x}(t)$ by a quadratic function (46), which can be considered constant provided we restrict ourselves to a time separation $t-t'$ small enough. One can always find a coordinate system $\{\mathbf{y}_i\}$ such that this quadratic potential reads:

$$\mathbf{Q}(\mathbf{y}) = \mathbf{Q}(0) + 1/2 \sum_i (\lambda_i - \mathcal{S}) y_i^2, \tag{58}$$

where the coordinates $\mathbf{y}$ must not be confused with the original coordinates $\mathbf{x}$ of the relaxational motion.

This section demonstrates that when a particle diffuses, or relaxes in such a parabolic potential, then a characteristic time t_f scaling like $\mathcal{S}^{-1}$ arises, which turns out to be the time scale along which the function $\overline{T}(t,t')$ departs from its equilibrium value 0, *i.e.* the fluctuation-dissipation violation characteristic time.

We consider a particle moving in the potential (58), starting at t_0, and define the time difference $\tau = t - t_0$. The intermediate steps of the calculation make use of τ, t_0, while the final results are expressed in term of t, t', in relation with the original problem.

Let us consider the same local average $\lceil \mathbf{y}_i^2(\tau) \rfloor$ as in equation (48). The $\mathbf{y}_i$ are related to the gradient's coordinates by $\boldsymbol{\gamma}_i(\tau) = -(\lambda_i - S) y_i(\tau)$:

$$\lceil y_i^2(\tau) \rfloor = \frac{g(\lambda, t_0+\tau)}{(\lambda - \mathcal{S})^2}\,. \tag{59}$$

The initial conditions $\lceil y_i^2(\tau=0) \rfloor$ are given by $g(\lambda, t_0)$. We compute the fluctuation dissipation violation $\overline{T}(t,t')$, when the quadratic potential (58) does not evolve with time ($\mathcal{S}$ fixed once for all), and with initial conditions arising from a realistic distribution $g(\lambda, t_0) = \Gamma \hat{G}(\lambda/\mathcal{S})$.

$$y_i(\tau) = y_i(0)\ \mathrm{e}^{-(\lambda_i - \mathcal{S})(\tau)}. \tag{60}$$

The distribution $g(\lambda, t_0+\tau)$ evolves like $\lceil \mathbf{y}_i^2(\tau) \rfloor \cdot (\lambda - \mathcal{S})^2$. One has, for all $t > t_0$:

$$\begin{aligned} g(\lambda, t_0+\tau) &= g(\lambda, t_0)\ \mathrm{e}^{-2(\lambda-\mathcal{S})(\tau)}; \\ \partial_t\ g(\lambda, t) &= -2 g(\lambda, t)(\lambda - \mathcal{S}). \end{aligned} \tag{61}$$

The usual response $r(t,t') = N^{-1} \sum_i \delta y_i(t)/\delta\zeta_i(t')$, and correlation $b(t,t') = N^{-1} \sum_i (y_i(t) - y_i(t'))^2$ functions re-express in terms of $g(\lambda, t')$:

$$r(t,t') = \int \mathrm{d}\lambda\ \rho(\lambda)\ \mathrm{e}^{-(\lambda-\mathcal{S})(t-t')}; \tag{62}$$

$$b(t,t') = \int \mathrm{d}\lambda\ \rho(\lambda) g(\lambda, t') \left(\frac{1 - \mathrm{e}^{-(\lambda-\mathcal{S})(t-t')}}{\lambda - \mathcal{S}} \right)^2; \tag{63}$$

$$\begin{aligned} \partial_{t'} b(t,t') &= -2 \int \mathrm{d}\lambda\ \rho(\lambda)\ g(\lambda, t') \left(\frac{1 - \mathrm{e}^{-(\lambda-\mathcal{S})(t-t')}}{\lambda - \mathcal{S}} \right); \\ &= -2\overline{T}(t,t'). \end{aligned} \tag{64}$$

By inserting $g(\lambda, t'=t_0) = \Gamma \hat{G}(\lambda/\mathcal{S})$ in (64), one finds the short time ($\tau \ll \mathcal{S}^{-1}$) result for $\overline{T}(t,t')$,

$$\overline{T}(t,t') = (t-t')\Gamma\mathcal{S}^{3/2}, \tag{65}$$

and the intermediate time one ($\tau \sim \mathcal{S}^{-1}$),

$$\begin{aligned} r(t,t') &= \mathcal{S}^{3/2} \Phi_0(\mathcal{S}(t-t')), \\ b(t,t') &= -2\Gamma\mathcal{S}^{1/2} \Phi_1(\mathcal{S}(t-t')), \\ \overline{T}(t,t') &= \frac{\Gamma}{\mathcal{S}} \frac{\Phi_0}{\Phi_1}(\mathcal{S}(t-t')). \end{aligned} \tag{66}$$

Φ_0,Φ_1 are smooth scaling functions written in Appendix B. Equation (66) shows that $\mathcal{S}^{-1}$ plays the role of a characteristic time for the onset of the effective temperature $\overline{T}$.

Assuming now the very likely value $\kappa = 2/3$ and $\Gamma = \mathcal{S}$, one finds that $\overline{T}$ takes a value of order one after a time interval $t_f \sim \mathcal{S}^{-1}$. We conclude that the characteristic time t_f scales like $t_f = t^\alpha \propto t^\kappa$, and $\alpha = \kappa = 2/3$. Our numerics (Fig. 4) leads to an estimated value $\alpha \simeq 0.64$, while $\kappa \simeq 0.67$. While we haven't proved that κ is actually $2/3$, we find the agreement satisfactory, and believe that the above picture describes correctly the first stage of the violation of the "fluctuation-dissipation relation at zero temperature".

How long can the quadratic approximation (46) accurately describes the original relaxational process? As $\mathcal{S}(t)$ decreases algebraically, the typical time δt to get $|\mathcal{S}(t+\delta t) - \mathcal{S}(t)| \sim \mathcal{S}(t)$ is t itself. More seriously, we have seen in the previous section that the unit vector of the trajectory $\dot{\mathbf{x}}(t)$ changes with the time scale $\mathcal{S}^{-1}$. As this change is somewhat related to the frame's chaotic motion, we deduce than $\mathcal{S}^{-1}$ must be an upper limit of validity for the quasi-static approximation. Finally, the relaxation on the saddle becomes ill-defined when $\mathcal{S}(t-t') \gg 1$, due to the exponential divergence of the functions $r(t,t')$ and $b(t,t')$, given by equations (62, 63). We reach the conclusion that this quasi-static picture breaks down for times larger than $\mathcal{S}^{-1}$, but provides a strong evidence in favour of $t_f(t) \sim \mathcal{S}^{-1}(t) \sim t^{2/3}$, in good agreement with our numerical findings (Sect. 3 and Fig. 4).

Let us close this section by computing the typical distance covered during a time interval $t - t' < \mathcal{S}^{-1}$, with a gradient coordinates distribution $g(\lambda, t') = \Gamma \hat{G}(\lambda/\mathcal{S})$.

$$\begin{aligned} b(t,t') &= \Gamma \mathcal{S}^{3/2} (t-t')^2 \\ &= \mathcal{S}^{5/2} (t-t')^2 \quad \text{if} \quad \kappa = 2/3. \end{aligned} \tag{67}$$

For a time interval $(t-t') \sim \mathcal{S}^{-1}$, one has $b(t,t') \sim \Gamma \cdot \mathcal{S}^{-1/2} \ll 1$, becoming $b(t,t') \sim \mathcal{S}^{1/2}$ for $\kappa = 2/3$. As $\mathcal{S}^{1/2}$ tends to zero, the characteristic time t_b of the evolution of $b(t,t')$ in the aging regime, is necessarily much greater than $t_f \sim \mathcal{S}^{-1}$.

7 A dynamics restricted to the downhill directions

This section shows how the above approach describes the long time aging regime.

The equation (54) has a simple physical interpretation. The only non-vanishingly small components γ_i of $-\boldsymbol{\nabla} V$ are those corresponding to $\lambda_i \leq \mathcal{S}$. Only a number $N \int_0^{\mathcal{S}} \mathrm{d}\lambda \rho(\lambda) \sim N\mathcal{S}^{3/2}$ directions i are contributing to $-(\boldsymbol{\nabla} V)^2 = -\sum_i \boldsymbol{\gamma}_i^2$. Each one of these $\boldsymbol{\gamma}_i$ has a magnitude of order $\boldsymbol{\gamma}_i^2 \sim \Gamma$. As a result, $N\dot{\mathcal{E}}$ scales like $-\sum_i \boldsymbol{\gamma}_i^2 = N\mathcal{S}^{3/2}\Gamma$.

$$\dot{\mathcal{E}} \propto -(\mathcal{E}(t) - \mathcal{E}_{\mathrm{d}})^{1+1/\kappa}. \tag{68}$$

The relaxation dynamics looks like if it was controlled by the difference $\mathcal{E}(t) - \mathcal{E}_{\mathrm{d}}$.

7.1 The linear response regime

A constant force $\mathcal{F}$ is now applied, uncorrelated to the potential V. Each one of its (comoving) coordinates f_i is random, time-dependent as the frame rotates during the particle's motion, and has a magnitude $f_i \sim F$. We suppose F weak enough to be considered as a perturbation.

At any time, there are "open", or downhill directions, with $\lambda_i \leq \mathcal{S}$ and "close", or uphill directions with $\lambda_i \geq \mathcal{S}$. The close directions behave as confining harmonic potentials which prevent the (weak) force f_i to drive the particle along this direction. The open directions are the one which drive the particle away. As the particle moves, "open" and "close" directions exchange their role, but the proportion of open directions remains proportional to $\mathcal{S}^{3/2}$.

The force $\mathcal{F}$ induces a displacement $\dot{\mathbf{x}}$ whose components are $\dot{\mathbf{x}}_i \simeq f_i$ along an open direction and $\dot{\mathbf{x}}_i \simeq 0$ along a close direction . The average velocity $\dot{\mathbf{x}}\mathcal{F}/\|\mathcal{F}\|$ is given by (θ Heaviside function):

$$\begin{aligned} \frac{\dot{\mathbf{x}}(t)\mathcal{F}}{\|\mathcal{F}\|} &\simeq \sum_i f_i^2 \; \theta(\mathcal{S} - \lambda_i)/\|\mathcal{F}\|; \\ &= N\mathcal{S}^{3/2}F^2/(\sqrt{N}F); \\ &= \sqrt{N}\; F\; \mathcal{S}^{3/2}; \end{aligned} \tag{69}$$

that we identify to $\sqrt{N}\; \dot{u}(t)$. As a result, one finds a velocity proportional to the number of downhill directions:

$$\dot{u} \propto F\mathcal{S}^{3/2}. \tag{70}$$

Inserting the likely value $\kappa = 2/3$, one finally gets a displacement $u(t) - u(t') \propto F(\ln(t) - \ln(t'))$, well confirmed by the numerics (Sect. 3 and Fig. 6). This pure relaxational motion is driven by the components $\boldsymbol{\gamma}_i$ of $-\boldsymbol{\nabla} V$, while the external force acts through f_i. One expects the linear response to hold while f_i^2 is smaller than $\boldsymbol{\gamma}_i^2$, but to break down as soon as $f_i^2 \simeq \boldsymbol{\gamma}_i^2$. This leads to a predicted cross-over time t_F, scaling like $\Gamma(t_F) = F^2$, or $t_F \sim F^{4/(\kappa-1)}$ [11].

7.2 The diffusive regime

The asymptotic behaviour predicted for $b(t,t')$ is, from equations (21–23):

$$b(t,t') = \frac{t-t'}{t_b} + \mathcal{O}\left(\frac{t-t'}{t_b}\right)^2. \tag{71}$$

One recognizes a simple diffusive behaviour, with effective diffusivity t_b^{-1}. From Section 6, we know that the short-time motion $(t-t') \leq \mathcal{S}^{-1} \sim t_f$ is ballistic, and that the particle covers a distance of $\Gamma\mathcal{S}^{-1/2}$. On the other hand, our Section 5 shows that the direction $\mathbf{w}$ of the trajectory $\mathbf{x}(t)$ uncorrelates after this same time $\mathcal{S}^{-1}$. Using a well-known result on correlated random walks, and assuming a free diffusive behaviour at intermediate times $t - t' \sim t_b$, as inferred by equation (71), one finds:

$$b(t,t') \simeq \left(\frac{t-t'}{\mathcal{S}^{-1}}\right)\left(\frac{\Gamma}{\sqrt{\mathcal{S}}}\right). \tag{72}$$

This corresponds to ballistic steps of length $(\Gamma/\sqrt{\mathcal{S}})$ (67), and a cross-over time from ballistic to diffusive regime equal to $\mathcal{S}^{-1}$. As $t_f \simeq \mathcal{S}^{-1}$,

$$b(t,t') \simeq (t-t')\Gamma\mathcal{S}^{1/2}, \tag{73}$$

leading to the identification:

$$\begin{aligned} t_b &\propto \Gamma^{-1}\mathcal{S}^{-1/2}; \\ &\propto \mathcal{S}^{1/\kappa}. \end{aligned} \tag{74}$$

If κ is taken equal to $2/3$, one gets $t_b \sim t' \sim t$.

Let us give reasons to be confident in the scaling $t_f \sim \mathcal{S}^{-1}$, $t_b \sim \mathcal{S}^{-3/2}$ and $\mathcal{S} \sim t^{-2/3}$. First, a matching argument similar to [10,13] predicts $t_b \sim t_f^{3/2}$. Then, the result $t_b \sim t'$ is in agreement with the conjecture $h(t) \sim t^{\delta}$. This entails a logarithmic growth of $b(t,t')$, t' fixed, and we have asymptotically (*i.e.* $t, t' \gg 1$, and $t/t' \sim 1$) a free Brownian motion in logarithmic time.

$$b(t,t') = \delta(\ln t - \ln t'). \tag{75}$$

This makes $\exp(-b(t,t'))$ as well as $r(t,t')$ decaying as a power law. While we have no demonstration, we think that a power-law decay of the memory function $f(b(t,t'))r(t,t')$ is necessary for the "fine tuned" aging solution of the system (8). Asking for a power-law decay $f(b(t,t'))$ in turn fixes κ to $2/3$.

Finally, if $\kappa = 2/3$, $t_b = \mathcal{S}^{-3/2}$, and the characteristic times for the linear response regime $\dot{u}(t) \simeq F/t_b$, and for the diffusion regime $b(t,t') \simeq (t-t')/t_b$ are the same, which is consistent with the persistence of an "Einstein relation" at the beginning of the aging regime.

8 Conclusion

We have proposed a geometrical description of the mean-field relaxational dynamics of a particle, for a subclass of short-range correlated disorders. We have restricted ourselves to the isolated case, and to the driven case in the linear response regime.

A numerical integration of the mean-field equations gives evidence of a power-law decay of the dynamical energy with an exponent κ numerically close to 2/3. We also found evidence of a logarithmic growth $b(t,t') \sim \ln t$ consistent with the conjecture $h(t) \sim t^{\delta}$ for the reparametrization function h.

The exponential correlator makes it possible to compute the density of eigenvalues of the Hessian $\mathcal{H}$ associated to the random potential, and we were able to predict the correct value (*i.e.* -2) of the dynamical energy $\mathcal{E}_{\rm d}$. Introducing a comoving frame, reminiscent from the INM frame of a supercooled liquid, we derive an expression for the distribution $g(\lambda,t)$ of the components of $\boldsymbol{\nabla} V\big(\mathbf{x}(t)\big)$. This expression is $g = \Gamma\ \hat{G}(\lambda/\mathcal{S})$, where $-\mathcal{S}(t)$ is the (time dependent) lowest eigenvalue of Spec($\mathcal{H}$).

For reasons exposed in Section 7, namely the consistence with $h(t) \sim t^{\delta}$, the requirement that $f(b)$ is likely to decrease as a power law, and acknowledging the numerical estimate of κ, we believe that κ is indeed equal to 2/3. This leads to the following predictions:

(1) $\Gamma \propto S$, and a typical gradient coordinate is, along a downhill direction, $|\gamma_i| \sim \sqrt{S} \sim t^{-1/3}$.

(2) From a short time, harmonic expansion of the particle's motion the characteristic time t_f leading to the appearance of an effective temperature goes like $t_f \sim S^{-1} \sim t^{2/3}$.

(3) The characteristic time at the beginning of the aging regime is $t_b \sim S^{-3/2} \sim t$. Both linear response $\dot{u} \sim F/t_b$ and diffusion $b(t,t') \sim (t-t')/t_b$ are controlled by it.

We observe that the aging mechanism of this model consists in a simultaneous decrease of the number of downhill directions (going like $NS^{3/2} \sim Nt^{-1}$) and of the typical gradient component $|\gamma_i| \sim t^{-1/3}$. We also predict that the effect of a constant force brings about a dramatic change in the dynamics after a time $t_F \sim F^{-3}$, reaching a out-of-equilibrium but stationary regime [11].

Finally, our geometrical analysis is satisfactory as far as the exponential correlator is concerned, but fails, under its present form, to describe the most generic situation.

I especially thank L. Cugliandolo and J. Kurchan for having lent me their numerical code, and S. Scheidl, J.P. Bouchaud, J. Kurchan, M. Mézard and A. Cavagna for discussions on this field. I thank D. Feinberg for suggestions and criticisms about the manuscript. I warmly thank the hospitality of the Department of Physics, IISc, Bangalore, where a part of the writing has been done.

Appendix A: The MSR action

The action leading to equations (8) is:

$$\begin{aligned} S[x,\mathrm{i}\tilde{x}] = \int_0^\infty \mathrm{d}t\ \Bigg\{ & -T\sum_{j=1}^{N}(\mathrm{i}\tilde{x}_j)^2(t) \\ & +\mathrm{i}\tilde{x}_1(t)(\dot{x}_1(t) - N^{1/2}F) + \sum_{j=2}^{N}\mathrm{i}\tilde{x}_j(t)\dot{x}_j(t) \Bigg\} \\ + \int_0^\infty \mathrm{d}t\ \mathrm{d}s\ \Bigg\{ & f'(d(t,s))\sum_{j=1}^{N}\mathrm{i}\tilde{x}_j(t)\mathrm{i}\tilde{x}_j(s) \\ & +4f''(d(t,s))\ r(t,s)\sum_{j=1}^{N}\mathrm{i}\tilde{x}_j(t)(x_j(t)-x_j(s)) \Bigg\}, \end{aligned} \tag{76}$$

and the expectation value of an observable $\mathcal{O}[x(t),\mathrm{i}\tilde{x}(t)]$, averaged over the disorder, is given by:

$$\overline{\langle\, \mathcal{O}\,\rangle} = \int \mathcal{D}x[t]\ \mathcal{D}\tilde{x}[t]\ \mathcal{O}\ \exp(-S). \tag{77}$$

Appendix B: The spectrum of the Hessian H

We consider $\overline{\delta(V(\mathbf{r})-V_0)\ \mathrm{Spec}(\mathcal{H})(\mathbf{r})}$ for any arbitrary potential. $V_0 = N\mathcal{E}$ is fixed, and the $\mathcal{H}_{ij} = \partial^2_{ij}V(\mathbf{r})$ are $N(N+1)/2$ Gaussian random variables. The correlations among the $\mathcal{H}_{ij}$ are listed in equation (34). We define the self-averaging quantity $\mathcal{D} = N^{-1}\sum_i \partial_{ii}V(\mathbf{r})$ so that:

$$\begin{aligned} N\overline{(\partial_{ii}V(\mathbf{r})-\mathcal{D})^2} &= 8f''(0) - 8f''(0)/N, \\ N\overline{(\partial_{ii}V(\mathbf{r})-\mathcal{D})V(\mathbf{r})} &= 0, \\ N\overline{(\partial_{ii}V(\mathbf{r})-\mathcal{D})(\partial_{jj}V(\mathbf{r})-\mathcal{D})} &= -8f''(0)/N, \\ &= 0 + \mathcal{O}(N^{-1}). \end{aligned} \tag{78}$$

The Hessian is now $\mathcal{H}_{ij} = \mathcal{D}\delta_{ij} + \mathcal{H}'_{ij}$. $\mathcal{H}'$ is a matrix of independent Gaussian centred random numbers. The diagonal elements are slightly correlated (of order $1/N^2$) and have a different variance than the off-diagonal elements, but this does not prevent the Wigner result to apply and the spectrum of $\mathcal{H}'$ is a centred semi-circle of width $\Lambda = 4\sqrt{f''(0)}$.

The determination of $\mathcal{D}$ follows from the fact that $\mathcal{E}$ and $\mathcal{D}$ are Gaussian distributed, with correlations:

$$\begin{aligned} N\overline{\mathcal{E}^2} &= f(0); \\ N\overline{\mathcal{D}^2} &= 4\left(\frac{N+2}{N}\right)f''(0); \\ N\overline{\mathcal{D}\cdot\mathcal{E}} &= 2f'(0). \end{aligned} \tag{79}$$

The joint probability distribution of $\mathcal{E}$ and $\mathcal{D}$ is:

$$\mathcal{P}(\mathcal{D},\mathcal{E}) = \frac{N}{2\pi\sqrt{cf(0)}}\exp\left(-\frac{N}{2}\left[\frac{\mathcal{E}^2}{f(0)}+\frac{(\mathcal{D}-a\mathcal{E})^2}{c}\right]\right);$$
$$c = \frac{4}{f(0)}(f(0)f''(0)-f'(0)^2)+\frac{8}{N}f''(0);$$
$$a = \frac{2f'(0)}{f(0)}. \quad (80)$$

Fluctuations of $\mathcal{D}$ are of order $N^{1/2}$ around its saddle point value $2f'(0)/f(0)\mathcal{E}$. It follows that Spec($\mathcal{H}$) is a semi-circle of radius Λ shifted by an amount $\mathcal{D} = 2f'(0)/f(0)\ \mathcal{E}$.

Let us consider now $\overline{\delta(V(\mathbf{r})-V_0)\delta(V(\mathbf{r}_1)-V_1)\mathrm{Spec}(\mathcal{H})(\mathbf{r})}$. This simple average measures the non-locality of Spec($\mathcal{H}$), *i.e.* its dependence on the values taken by the random potential $V(\mathbf{r}')$ around $\mathbf{r}$.

The rotational invariance of the above average is broken, and $\mathbf{r}-\mathbf{r}'$ plays a special role. We relabel hereafter the direction 1 to coincide with $\mathbf{r}-\mathbf{r}'$, and define $b = \|\mathbf{r}-\mathbf{r}'\|^2/N$. Correlations are now, in addition to (34),

$$\overline{\partial_{ii}V(\mathbf{r})V(\mathbf{r}')} = 2f'(b) \quad \text{if } i\geq 2;$$
$$\overline{\partial_{11}V(\mathbf{r})V(\mathbf{r}')} = 2f'(b)+4bf''(b);$$
$$\overline{\partial_{ij}V(\mathbf{r})V(\mathbf{r}')} = 0. \quad (81)$$

$\mathcal{D}$ is again defined as $N^{-1}\sum_i \partial_{ii}V(\mathbf{r})$ and $\mathcal{H}'_{(i,j)\geq 2}$ is equivalent to the above situation: independent, centred, Gaussian random components, and the spectrum is a centred semi-circle. Adding one row and one column of random independent elements to $\mathcal{H}'_{(i,j)\geq 2}$ must not change the density profile of eigenvalues. This is because this eigenvalue distribution is a fixed point under the change $N\to N+1$, as argued in the "cavity" approach of the problem. A possible trouble comes from the single component $\partial_{11}V-\mathcal{D}$ which does not average to 0, but this does not alter the final result more than by a single isolated eigenvalue.

It is possible to show, with the help of a formal field theoretical approach, that the correlations (34, 81) indeed lead to the ordinary $N\to\infty$ saddle point for Spec($\mathcal{H}'$), *i.e.* a semi-circle law of radius Λ.

The computation of $\mathcal{D}$ follows closely the lines of the previous paragraph. We found that if $\mathcal{E} = V(\mathbf{r})/N$, $\mathcal{E}' = V(\mathbf{r}')/N$ and $b = \|\mathbf{r}-\mathbf{r}'\|^2/N$, then:

$$\mathcal{D} = \left(\frac{f'(0)+f'(b)}{f(0)+f(b)}\right)(\mathcal{E}+\mathcal{E}') + \left(\frac{f'(0)-f'(b)}{f(0)-f(b)}\right)(\mathcal{E}-\mathcal{E}'). \quad (82)$$

For a generic correlator, there is an explicit dependence on $\mathcal{E}'$ ("non locality") while for an exponential correlator $f = \exp(-y)$, the above formula reduces to $\mathcal{D} = 2f'(0)/f(0)\ \mathcal{E}$.

This suggests that the determination of Spec($\mathcal{H}$) from (29) is a complex problem and the simple behaviour (32) fails for a generic f.

The exponential correlator, however, has a strong property. The average:

$$N\overline{\left(\frac{2f'(0)}{f(0)}\mathcal{E}-\mathcal{S}\right)^2} = \frac{4}{f(0)}(ff''-f'^2)+\frac{8}{N}f''(0);$$
$$= \frac{8}{N}f''(0). \quad (83)$$

is 0 at the order N^{-1}. This means that, while b is strictly positive, there is no possible fluctuations of $\mathcal{D}$ around $2f'(0)/f''(0)\ \mathcal{E}$.

Repeating the argument for (37), n finite, shows that Spec($\mathcal{H}$) depends only on $V(\mathbf{r})$ and not on its local environment. Thus, we argue that the average (29) is given by (31, 32), as announced.

Appendix C: The quasi-static picture

From equation (62), we derive the expression for $r(t'+\tau,t')$.

$$r(t'+\tau,t') = 2\frac{\mathrm{e}^{\mathcal{S}\tau}\ \mathrm{I}_1(\Lambda\tau)\ \mathrm{e}^{-\Lambda\tau}}{\Lambda\tau}, \quad (84)$$

where I_1 is the modified Bessel function of first kind. The short time expansion of (64) is:

$$\partial_{t'}b(t'+\tau,t') = -2\tau\int \mathrm{d}\lambda\ \rho(\lambda)g(\lambda,t');$$
$$= -2\tau\Big(\dot{\mathcal{E}}(t')\Big)^2;$$
$$= -2\tau\ \Gamma S^{3/2}. \quad (85)$$

In the intermediate time separation regime, τ is of order $\mathcal{S}^{-1}$. The integral is dominated by $\lambda\sim\mathcal{S}$ and cut off by $g(\lambda,t')$ for $\lambda\mathcal{S}\gg 1$. $\rho(\lambda)$ can be replaced by its $\lambda\to 0$ equivalent.

$$r(t'+\tau,t') \simeq \sqrt{2/\pi}\mathrm{e}^{\mathcal{S}\tau}(\Lambda\tau)^{-3/2};$$
$$= \mathcal{S}^{3/2}(\sqrt{2/\pi}\Lambda^{-3/2})(\mathcal{S}\tau)^{-3/2}\mathrm{e}^{\mathcal{S}\tau};$$
$$= \mathcal{S}^{3/2}\Phi_0(\mathcal{S}\tau). \quad (86)$$

$$\partial_{t'}b(t'+\tau,t') = -2\Gamma\mathcal{S}^{1/2}\int_0^{2\Lambda/\mathcal{S}\simeq\infty}\mathrm{d}u\ (2/\Lambda)^{3/2}\pi^{-1}\sqrt{u} \times\hat{G}(u)\left(\frac{1-\mathrm{e}^{-\mathcal{S}\tau(u-1)}}{u-1}\right);$$
$$= -2\Gamma S^{1/2}\Phi_1(\mathcal{S}\tau). \quad (87)$$

The effective temperature behaves as:

$$\overline{T}(t'+\tau,t') = \left(\frac{\Gamma}{\mathcal{S}}\right)\frac{\Phi_1(\mathcal{S}\tau)}{\Phi_0(\mathcal{S}\tau)}, \quad (88)$$

reducing to

$$\overline{T}(t,t') = \frac{\Phi_1}{\Phi_0}(\mathcal{S}(t-t')), \quad (89)$$

if $\kappa = 2/3$ and $\Gamma = \mathcal{S}$.

References

1. D. Sherrington, S. Kirkpatrick, Phys. Rev. Lett. **35**, 1792 (1975); M. Mézard, G. Parisi, M.A. Virasoro, *Spin glass theory and beyond* (World Scientific, Singapore, 1987).
2. A. Crisanti, H. Horner, H. Sommers, Z. Phys. B **92**, 257 (1993).
3. L. Cugliandolo, J. Kurchan, Phys. Rev. Lett. **71**, 173 (1993).
4. For instance, the molecular dynamics of a Lennard-Jones fluid: J.L. Barrat, W. Kob, J. Phys. Cond. Matt. **11**, A247 (1999), or some finite dimensional spin glasses: E. Marinari, G. Parisi, F. Ricci-Tersenghi, J.J. Ruiz-Lorenzo, J. Phys. A **31**, 2611 (1998).
5. J.-P. Bouchaud, L. Cugliandolo, J. Kurchan, M. Mézard, in *Spin Glasses and Random Fields*, edited by A. Young (World Scientific, Singapore, 1997).
6. T.R. Kirkpatrick, P.G. Wolynes, Phys. Rev. A **35**, 3072 (1986); T.R. Kirkpatrick, D. Thirumalai, Phys. Rev. B **36**, 5388 (1987).
7. J. Kurchan, L. Laloux, J. Phys. A **29**, 1929 (1996).
8. S. Franz, M. Mézard, Europhys. Lett. **26**, 209 (1994); Physica A **210**, 48 (1994).
9. L. Cugliandolo, P. Le Doussal, Phys. Rev. E **53**, 1525 (1996).
10. H. Horner, Z. Phys. B **100**, 243 (1996).
11. F. Thalmann, Eur. Phys. J. B **19**, 65 (2001).
12. C. De Dominicis, Phys. Rev. B **18**, 4913 (1978); P. Martin, E. Siggia, H. Rose, Phys. Rev. A **8**, 423 (1973).
13. H. Kinzelbach, H. Horner, J. Phys. I France **3**, 1329 (1993).
14. We refer here to the mode coupling equations for supercooled liquids, as reviewed in [15].
15. W. Götze, in *Liquids, freezing and glass transitions*, *Les Houches Summer School*, edited by J. Hansen, D. Lesveque, J. Zinn-Justin (North Holland, 1989), p. 287; W. Götze, L. Sjögren, Rep. Prog. Phys. **55**, 241 (1992).
16. J.-P. Bouchaud, L. Cugliandolo, J. Kurchan, M. Mézard, Physica A **226**, 243 (1996).
17. L. Cugliandolo, J. Kurchan, J. Phys. A **27**, 5749 (1994).
18. L. Cugliandolo, J. Kurchan, L. Peliti, Phys. Rev. E **55**, 3898 (1997); S. Franz, M.A. Virasoro, J. Phys. A **33**, 891 (1999).
19. B. Kim, A. Latz, `cond-mat/0005172`; H. Horner (private communication).
20. G. Biroli, J. Phys. A **32**, 8365 (1999); J. Phys. Cond. Matt., **12**, 6375 (2000) `cond-mat/0003234`.
21. T. Keyes, J. Phys. Chem. A **101**, 2921 (1997).
22. A. Cavagna, I. Giardina, G. Parisi, Phys. Rev. B **57**, 11251 (1998).
23. A. Crisanti, H. Sommers, Z. Phys. B **87**, 341 (1992).
24. J. Kurchan, G. Parisi, M. Virasoro, J. Phys. I France **3**, 1819 (1993).
25. S. Franz, G. Parisi, J. Phys. I France **5**, 1401 (1995).
26. A. Cavagna, I. Giardina, G. Parisi, J. Phys. A **30**, 4449 (1997).
27. A. Barrat, R. Burioni, M. Mézard, J. Phys. A **29**, L81 (1996).
28. K. Broderix *et al.*, Phys. Rev. Lett. **85**, 5360 (2000) `cond-mat/0007258`.